

Simulation of Track and Landfall Process of Severe Cyclonic Storm Mora over the Bay of Bengal using WRF-ARW Model

Most. Fatema Amin Akhi^{1*}, Md. Saddam Hossain², Md. Shakil Hossain³ and Muhammad Abul Kalam Mallik⁴

¹Department of Mathematics, Dhaka University of Engineering and Technology, Gazipur-1707, Bangladesh

²Department of Mathematics, Bangladesh University of Engineering and Technology, Dhaka-1000, Bangladesh

³Department of Mathematics, Khulna University of Engineering & Technology, Khulna-9203, Bangladesh

⁴Bangladesh Meteorological Department, Dhaka-1207, Bangladesh

(Received : 20 February 2023; Accepted : 20 July 2023)

Abstract

The simulations of Severe Cyclonic Storm (SCS) Mora (28-31 May 2017) generated over the Bay of Bengal (BoB) are performed in this study to analyze its features, landfall, and track using the Weather Research and Forecasting (WRF) model. WRF-ARW model has been used on a 10 km Horizontal Resolution (HR) domain for 96, 72, 48, and 24-hour lead time simulations. The model's performance is assessed by examining Mean Sea Level Pressure (MSLP), vertical distribution of velocity components, wind flow pattern, relative vorticity, vertical wind shear, relative humidity, latent heat flux at the surface, and track pattern. The simulated results are compared carefully to the observations from the Bangladesh Meteorological Department (BMD) and the India Meteorological Department (IMD). The findings are reasonably consistent with the observations. The simulated track is also reasonable even up to 72 hours in advance. Finally, the study's results suggest that the WRF model can be used as an effective tool in predicting TCs over the BoB.

Keywords: Tropical cyclone, track, landfall, Mora, Bay of Bengal

I. Introduction

Tropical Cyclones (TCs) are the most severe catastrophic events on Earth. Due to severe gale winds, heavy rainfall, and related storm surge, they cause significant devastation to life and property¹. Storm surges are mainly responsible for the significant loss of lives and properties. 90% of TC deaths are caused by storm surges which is the worst effect of the landfalling cyclone^{2,3}. Bangladesh suffers nearly 40% of the total worldwide storm surge effects. Due to the influences of climatic forcing, shallow bathymetry, strong astronomical tide, and the funneling structure of the Bay, the BoB and the Arabian Sea are the basins where TCs cause significant damage. Around 7% of the global yearly total number of TCs develop over the BoB. These climatological hazards, which develop from October to December, are extremely destructive, causing damage to life and property, especially when they strike the coastlines of Indian subcontinents^{4,5}. As a result, proper prediction of severe cyclones is essential for minimizing the loss of valuable lives and property⁶.

Several studies in TC forecasting have been performed over the last several decades, utilizing improved numerical techniques and operational cyclone forecasting. Pattanaik and Mohanty examined the suitability of the WRF and MM5 models in the prediction of TCs across the Indian Ocean. The result suggested that the WRF model generated results were similar to the observations, whereas MM5 simulated output was not fair enough⁷. It is also demonstrated that the WRF model is capable of simulating

the genesis, intensity, track, and landfall of TC reasonably well^{8,9,10}. Though the study of TCs has improved a lot, analyzing cyclone structure is still challenging in both operational and research fields. Some great researchers have developed different parameterization schemes but most of these schemes have certain limitations¹¹.

Atmospheric parameters such as Sea Surface Temperature (SST), Relative Vorticity (RV), Vertical Wind Shear (VWS), moisture distribution, and relative vorticity are crucial parameters for the severity of a TC¹². Relative Humidity (RH) distribution is a crucial factor that influences the structure of the TC¹³. The development of TC depends on heat from the rain bands¹⁴. Deshpande *et al.* studied the 'Odisha' super cyclone (1999) and suggested that the track and intensity are influenced by the Cumulus parameterization (CP) schemes utilized in the model. They also found that Kain-Fritsch (KF) scheme gives better track and intensity prediction than other schemes¹⁵. Mohanty *et al.*¹⁶ in 2010 simulated very severe cyclones over BoB with several initial and boundary conditions of the WRF model and found that Final Analyses (FNL) data gives less error in landfall prediction than Global Forecast System (GFS) data. In Bangladesh, Akhter *et al.*¹⁷ conducted a comparative analysis between WRF and MM5 models to simulate TC 'Rashmi' and found the WRF model performs better than the MM5 model. Better forecast performance of the MM5 model was demonstrated than the RAMS model in simulating TCs across the BoB¹⁸. It is also found that using HRs is beneficial for the simulation of track and landfall characteristics of TCs throughout the BoB^{19,20}.

* Author for correspondence. e-mail: akhi@duet.ac.bd

The regions where a TC makes landfall are the most vulnerable areas. TC land falling events have a devastating impact on people's lives and property in the Indian subcontinent's coastal regions. Cyclones in the BoB are reported to be responsible for 61.6 million people being affected, 0.75 to 1.23 million lives lost, and \$4.7 to \$9 billion in losses in Bangladesh's coastal regions²¹. The civilization of these low-lying coastal regions is extremely concerned regarding the present and upcoming challenges to their way of living. Proper storm predictions may contribute to decreasing the impact of disasters throughout the regions. The main goal of this paper is to generate the potential variations in associated meteorological parameters both before and after a cyclone makes landfall, and to determine how such variations affect the storm's severity. It is believed that understanding the potential changes in the respective meteorological parameters will help to take appropriate measures to reduce the damage in the potential areas.

II. Synoptic Description of Tropical Cyclone Mora

A Low-Pressure Area (LPA) was developed across the southeast BoB and neighboring regions of central BoB in the early hours of the morning (0300 UTC) of May 25th, 2017. It continued throughout the same areas on the 26th May, and in the morning (0300 UTC) of the 27th May, it was regarded as a well-structured low-pressure system across the east-central and neighboring west-central and southeast BoB. It progressed north-eastwards direction in the early morning (0000 UTC) of May 28th, and deepened into a Depression (D) throughout east-central BoB. Moving northeastwards, it developed into a Deep Depression (DD) and subsequently a Cyclonic Storm (CS) MORA throughout east-central BoB in the afternoon (0900 UTC) and late evening (1800 UTC) of 28th May. Around the evening (1200 UTC) of May 29th, it advanced north-northeastwards and concentrated into a SCS. The system gained its highest intensity of Maximum Sustained Wind Speed (MSWS) of 60 knots and Estimated Central Pressure (ECP) of 978 hPa at 2100 UTC on 29th May. It continued to proceed north-northeastwards in the morning hours of the 30th May (around 0400 and 0500 UTC) and crossed the Bangladesh coastline near Chittagong. After hitting land, the system has begun to lose intensity quickly and becomes a CS, DD, and D at about 0900, 1200, and 1800 UTC on 30th May, respectively. It further degraded into a low-pressure system over Nagaland and the adjacent region, and became a LPA in the morning hours (0300 UTC), becoming less markable in the afternoon (0900 UTC)²².

III. Experimental Setup, Data Used, and Methodology

The National Centers for Environmental Prediction (NCEP) high-resolution FNL data on $1^\circ \times 1^\circ$ grid throughout the entire globe was used as the initial and lateral boundary condition in this study. The Terrain/Topography simulation was done using 30 seconds of United States Geological Survey (USGS) data, while the vegetation/land use coverage was done using 25 categories of USGS data. Among the different Numerical Weather Prediction (NWP) mesoscale models, the WRF model (Version 4.3.1) model is chosen in this study. The WRF model has been conducted for 24, 48, 72, and 96 hours lead time simulations using different initial and lateral boundary conditions. The model was set up on a single domain with a HR of 10 km. The model-simulated MSLP is compared to the ECP given in the IMD reports on SCS Mora²². The number of grid points was 240 in both X-direction (West-East) and Y-direction (South-North).

Table 1. Overview of WRF model configurations Dynamics and domain

WRF core	ARW
Data	NCEP-FNL
Interval	1 hour
Number of domains	1
Central point of the domain	17.5° N & 88° E
Covered area	8° – 27° N and 79° – 97° E
Horizontal grid distance	10 km
Integration time step	60 s
Map projection	Mercator
Vertical coordinate	Pressure coordinate
Time integration scheme	3 rd order Runge-Kutta
Spatial differencing scheme	6 th order centered differencing
Physics	
Microphysics	Kessler scheme ²³
Cumulus parameterization	Kain-Fritsch (new Eta) scheme ²⁴
PBL Parameterization	Yonsei University (YSU) scheme ²⁵
Surface layer physics	Revised MM5 scheme ²⁶
Land-surface model	Unified Noah LSM ²⁷
Short wave radiation	Dudhia scheme ²⁸
Long wave radiation	RRTM scheme ²⁹

IV. Results and Discussion

Analysis of MSLP

The formation of a LPA is a key process for potential weather disturbances that could progress into a TC if suitable climatological conditions exist. The simulated MSLP (hPa) of the SCS Mora valid at (the time of model

simulated landfall) 2300 UTC of 29th May, 0100 UTC of 30th May, 0100 UTC of 30th May, 0200 UTC of 30th May, 2017 based on the initial condition of 0000 UTC of 27th, 28th, 29th and 30th May, 2017 are presented in Fig. 1 (a-d) respectively. From the simulated MSLP analysis, it is found that a well-marked LPA is formed over east central & southeast BoB and it's moving north-northeastwards. It is found that the cyclone's center at the time of landfall, is located at 21.97^o N, 90.33^o E, 21.78^o N, 91.82^o E, 21.41^o N, 91.98^o E, and 21.6^o N, 91.95^o E respectively throughout the southeastern part of Bangladesh and adjacent regions based on 96, 72, 48, and 24-hours simulations.

It is also found that MSLP continually decreases with time and reaches its maximum intensity just before landfall, and then the pressure gradually rises. The MSLP of the system at the time of landfall is found 935, 955, 971, and 977 hPa respectively based on the 96, 72, 48, and 24-hour simulations. The simulated Lowest Central Pressure (LCP) of the SCS Mora is found 935 hPa at 2300 UTC of 29th May 2017 of 96 hours model run.

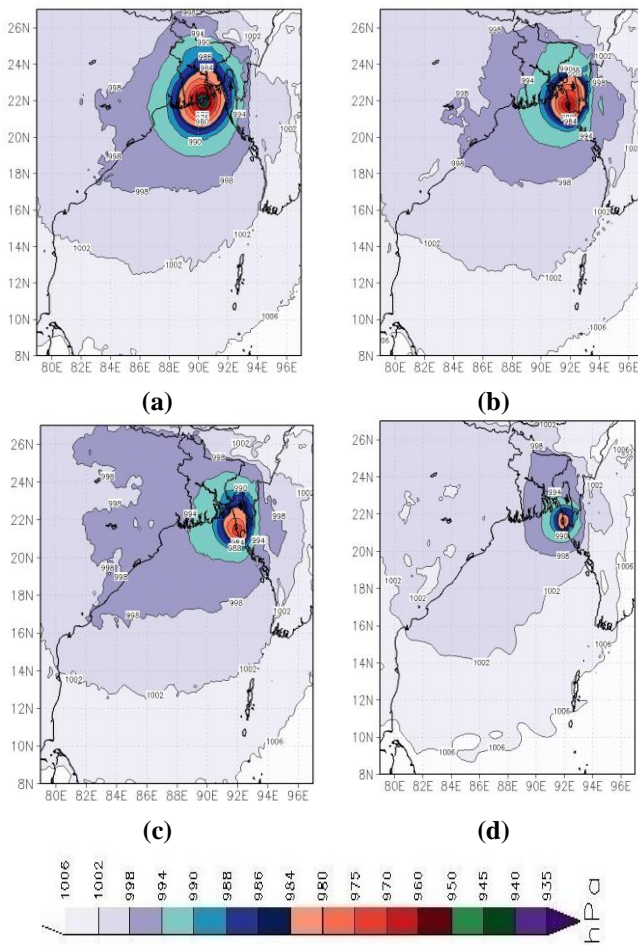


Fig. 1. The spatial distribution of MSLP (hPa) based on 0000 UTC of (a) 27, (b) 28, (c) 29, and (d) 30 May, 2017 respectively.

A comparison of the IMD's ECP²² and simulated LCP of the SCS Mora is presented in Fig. 2 (a-c) for 72-, 48-, and 24-hour simulations respectively. The ECP and the simulated MCP gradually decrease with time and reach its minimum just before the landfall. Model-simulated MCP falls more sharply than the observations.

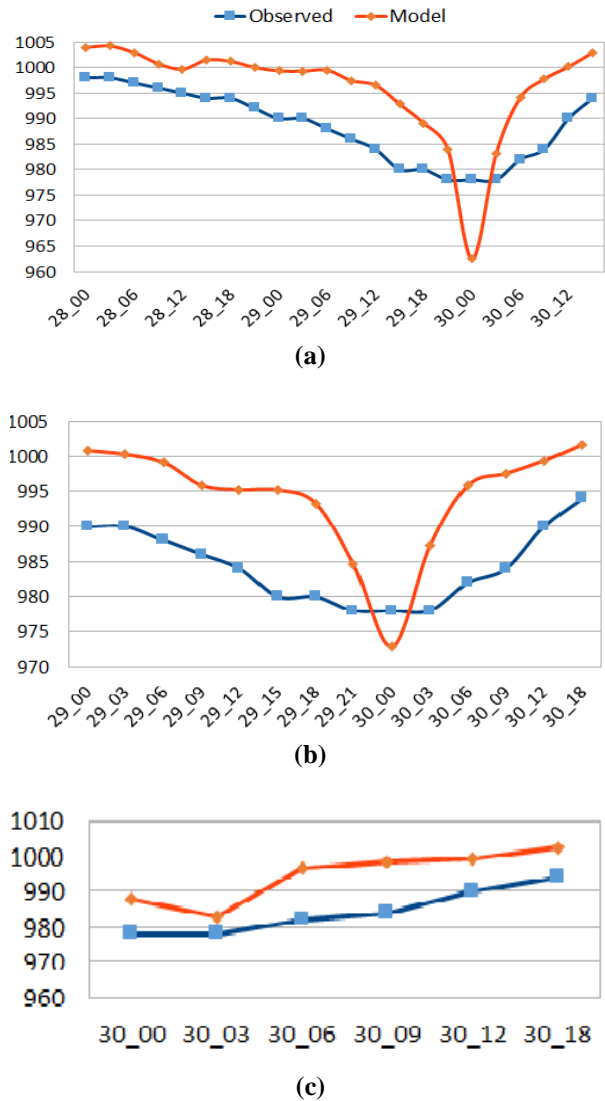


Fig. 2. Comparison of model simulated LCP (hPa) of TC Mora with the ECP (hPa) for (a) 72, (b) 48, and (c) 24-hour simulations.

Analysis of Wind at 850 hPa Level

The horizontal distributions of wind flow ($m s^{-1}$) at 850 hPa level of the TC Mora valid at 2300 UTC of 29th May, 0100 UTC, 0100 UTC, and 0200 UTC of 30th May, 2017 based on 96-, 72-, 48- and 24-hours simulations are displayed in Fig. 3 (a-d) respectively. From the simulated wind flow analysis, A significant cyclonic circulation has been simulated in each phase of the wind distribution which is the evidence in the inflow of wind at lower levels. A

cyclonic circulation is also predicted to prevail throughout Bangladesh's south-eastern coast and in the surrounding regions, according to the simulation results.

The distribution depicts a well-organized calm central region along with Several bands of wind around the center. The primary maximum wind of magnitude $50\text{-}55\text{ m s}^{-1}$ for both 96- and 72-hour model run and $40\text{-}45\text{ m s}^{-1}$ for both 48- and 24-hour simulations is determined in the southwest portion of the simulated system. The secondary maxima were found of magnitude $40\text{-}50\text{ m s}^{-1}$ for both 96- and 72-hour model run and $35\text{-}40\text{ m s}^{-1}$ for both 48- and 24-hour simulations in the southwest sector of the simulated system.

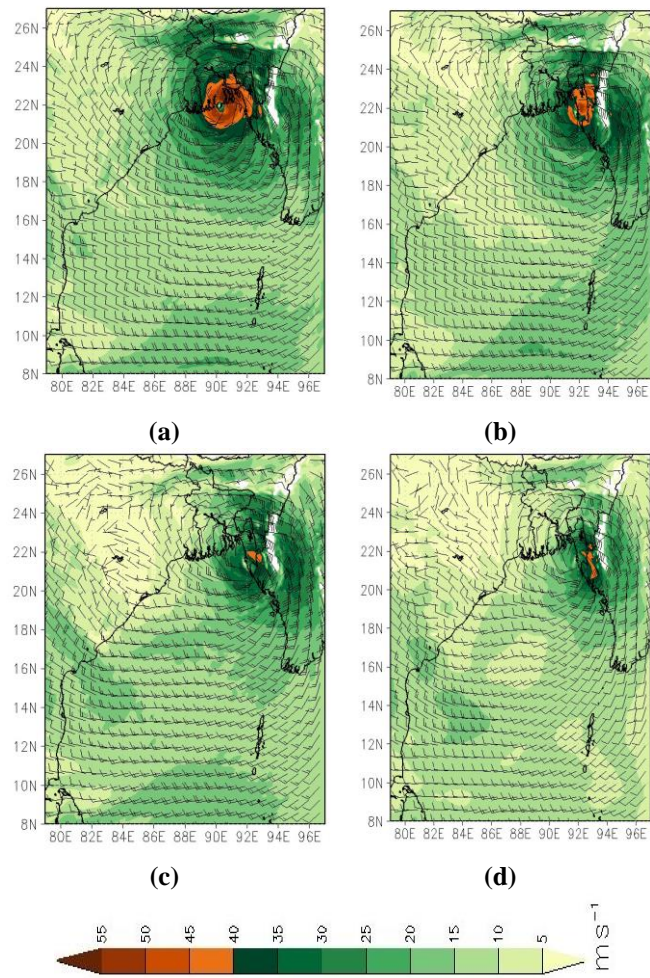


Fig. 3. The spatial distribution of wind flow (m s^{-1}) at 850 hPa level based on 0000 UTC of (a) 27, (b) 28, (c) 29, and (d) 30 May, 2017 respectively.

Analysis of Vertical Wind Shear

The Fig. 4 (a-d) represents the distributions of model-simulated VWS (m s^{-1}) between 200 hPa and 850 hPa (u component of wind) of the TC Mora at the time of model-simulated landfall for 96, 72, 48, and 24-hour simulations

respectively. The VWS at the center is nearly zero as the system's center is almost calm. But, the value of the VWS continues to rise throughout the regions surrounding the system center. The values of VWS are also seen to decrease as the system becomes more severe. Low VWS has been identified until the system reaches its maximal intensity stage. These small values are below 10 m s^{-1} and are convenient for the development of the system since weak VWS means there is very small vertical tilt of the system. A high VWS of about 30 m s^{-1} is noted in the TC's peripheral region near landfall time, promoting the development of extreme rainfall events across Bangladesh's south and southeast coasts and nearby areas. From the Figure, it is clear that, the value of VWS increases towards the outer periphery of the TC, particularly in the north-east direction.

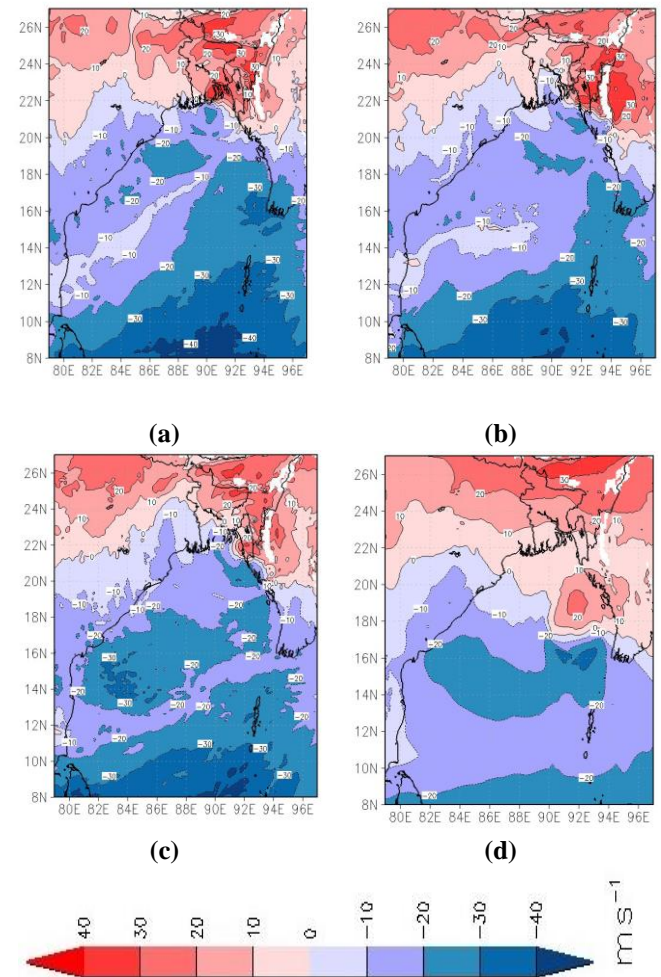


Fig. 4. The spatial distribution of VWS based on 0000 UTC of (a) 27, (b) 28, (c) 29, and (d) 30 May, 2017 respectively.

Analysis of the Zonal Component of Velocity

Fig. 5 (a-d) indicates the vertical distribution of zonal wind between 950-100 hPa level at longitude 91.98°E ; 90.98°E ;

91.82°E and 90.33°E (location of the system center) at the time of landfall for 96, 72, 48, and 24-hour simulations respectively. The distribution of zonal wind reveals that the wind speed is positive along the lower latitude and negative along the higher latitude of the system center. A positive value suggests that the direction of the wind is from west to east, whereas a negative value means that the direction of the wind is from east to west. From this analysis, it is found that the primary maximum wind is found in the southeast sector of the central region and it extends up to 100-150 hPa levels. A calm wind with a magnitude less than 5 m s^{-1} is found along the center of the system for all simulations. This calm central region is extended vertically which is like a hollow. Very strong winds are found around this calm central region on both sides of the system. These strong winds flow in an easterly direction (negative) in the northern sector of the central region and in a westerly direction (positive) in the southern side. These easterly and westerly winds indicate deep inflow in the lower level to mid-tropospheric level. Maximum wind of $40\text{-}50 \text{ m s}^{-1}$ is observed at the lower latitude of the system center and $10\text{-}30 \text{ m s}^{-1}$ wind is determined in the upper latitude for both 96- and 72-hour model run. MSWS of $20\text{-}40 \text{ m s}^{-1}$ is observed at the lower latitude of the system center and $10\text{-}20 \text{ m s}^{-1}$ wind is determined in the upper latitude for both 48- and 24-hour model run. But the vertical extension of this maximum wind on the northern side is up to 750 hPa level and on the southern side it is up to 300 hPa level. So, there is an asymmetry between the north and south sector of the system. Varying magnitudes of heavy winds are confined to various tropospheric levels which are shown by the decreasing values of winds with increasing height. It is also found that in the horizontal directions, the magnitudes of wind are also decreasing with increasing distance from the center.

Analysis of the Meridional Component of Velocity

Fig. 6 (a-d) indicates the vertical distribution of meridional wind from 950-100 hPa level at latitude 21.97°N; 21.42°N; 21.78°N and 21.97°N valid at the time of model simulated landfall for 96, 72, 48, and 24-hour simulations respectively. The meridional wind results demonstrated that wind speed is negative along the system center's lower longitude and positive along the system center's higher longitude. A positive value means that the direction of the wind is from south to north, whereas a negative value

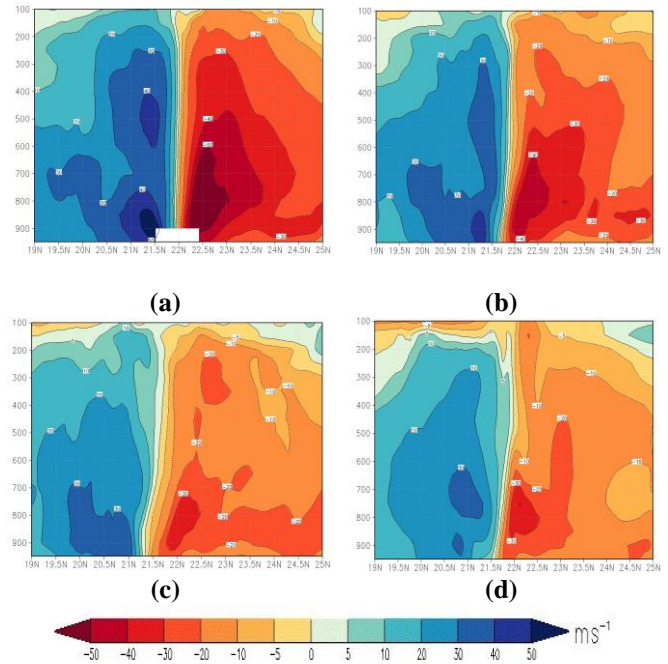


Fig. 5. The spatial distribution of zonal wind based on 0000 UTC of (a) 27, (b) 28, (c) 29, and (d) 30 May, 2017 respectively.

indicates that the direction of the wind is from north to south. The east-west sectional view of the meridional wind depicts a relatively calm central region with wind speed $0\text{-}5 \text{ m s}^{-1}$. Strong winds that encircle the calm central region have been found on both sides of the system. These strong winds flow in a southerly direction (positive) in the eastern sector of the system and in a northerly direction (negative) in the western side. These strong southerly and northerly winds indicate deep inflow in the lower level to mid-tropospheric levels. From this analysis, it is found that the primary maximum wind is found to the southeast sector of the system core and it extends up to 200 hPa level. The strong wind has one maximum of around $50\text{-}60 \text{ m s}^{-1}$ up to 300 hPa level to the east side for both 96 and 72-hour model run and other maxima of $40\text{-}50 \text{ m s}^{-1}$ up to 300-500 hPa to the west side of the central region. So, there is a lack of symmetry in the shape of the TC. The magnitudes of winds are decreasing with increasing height i.e., varying magnitudes of heavy winds are confined to various tropospheric levels. As the distance from the center increases, wind speed decreases in both horizontal directions.

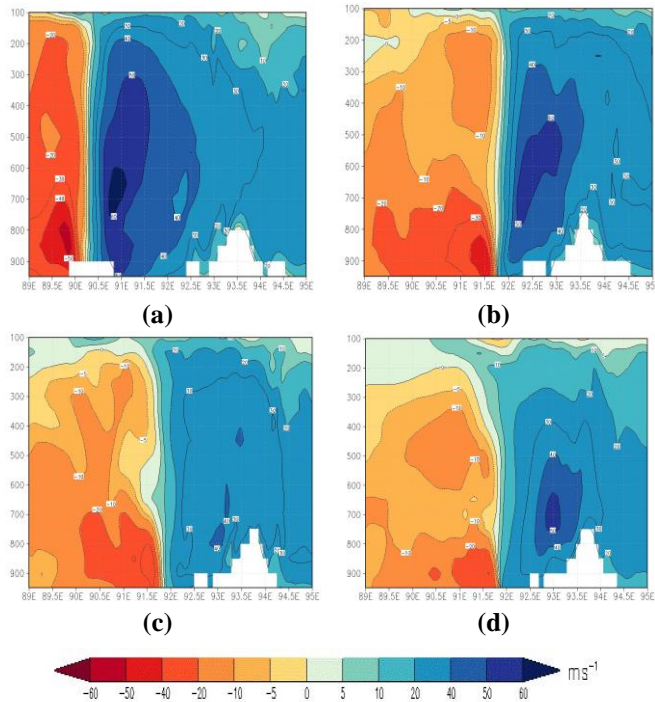


Fig. 6. The spatial distribution of meridional wind based on 0000 UTC of (a) 27, (b) 28, (c) 29, and (d) 30 May, 2017 respectively.

A strong wind of 30 m s^{-1} is found up to 300 hPa level to the east side of the system core for all simulations. So, the WRF model has captured the meridional wind reasonably well though some asymmetry was predicted.

Analysis of Relative Vorticity

Fig. 7 (a-d) represents the distribution of model-simulated RV ($\times 10^{-5} \text{ s}^{-1}$) of the TC Mora at the time model-simulated landfall for 96, 72, 48, and 24-hour simulations respectively. It is understood from the figures that the maximum RV is found from the center and it is positive for all the levels. The values of RV decrease as the distance from the center increases i.e., the vorticity is found to be lower in the surrounding region of the center than that of the center. Also, the values of positive RV increase with time i.e., the system is associated with increasing vorticity with the development of the TC. At the time of landfall, the RV is found around 240-270, 210-240, 150-210, and 120-150 $\times 10^{-5} \text{ s}^{-1}$ for 96, 72, 48, and 24-hour model runs respectively. At this stage, the RV maintains a circular pattern though there is a little asymmetry in the outer periphery. The negative vorticity is found to be far away from the system center. The circular pattern of distribution is well-organized with decreased asymmetry in the outer periphery in this stage.

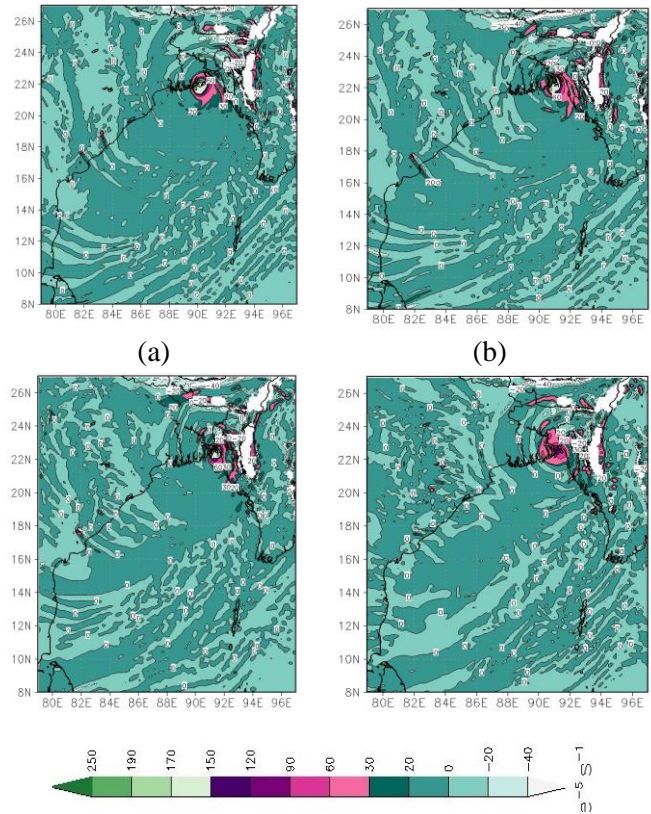


Fig. 7. The spatial distribution of RV based on 0000 UTC of (a) 27, (b) 28, (c) 29, and (d) 30 May, 2017 respectively.

It is determined that the vorticity around the system center is positive [$(20-60) \times 10^{-5} \text{ s}^{-1}$], which is very conducive to the development of deep convective clouds. Though it has some biases, the WRF model can generate the RV reasonably well even 96 hours in advance before landfall.

Analysis of Relative Humidity

The distributions of model-simulated RH of the TC Mora at the time of model-simulated landfall are shown in Fig. 8 (a-d) for 96, 72, 48, and 24-hour simulations, respectively. The analysis of simulated RH at 850 hPa level reveals that high RH (over 80%) existed across the simulated region, which progresses continuously to the northeast (southwesterly flow direction). A considerable southwesterly flow that transports a large quantity of moisture around 80-100 percent is also found over the south southeastern portion of Bangladesh and adjacent places. At the time of landfall, this high RH is responsible for the occurrence of convective activities associated with the cyclonic system that contributes to the progress of heavy rainfall events in these regions.

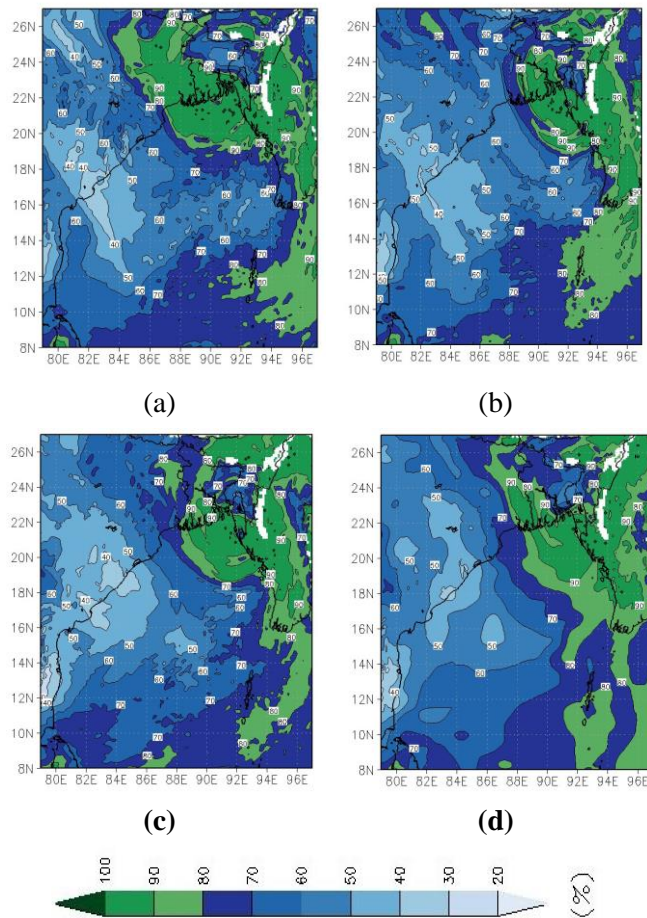


Fig. 8. The spatial distribution of RH based on 0000 UTC of (a) 27, (b) 28, (c) 29, and (d) 30 May, 2017 respectively.

Analysis of Latent Heat Flux

Fig. 9 (a-d) represents the distributions of model simulated Latent Heat Flux (LHF) associated with the TC Mora at the time of model-simulated landfall for 96, 72, 48, and 24-hour simulations respectively. The LHF is the minimum at the center, corresponding to a calm central region. In the formation stage, maximum LHF is found in the southern section of the system. The stronger LHF to the southwest sector of the system helps the system to move northeastward. As the system is over the Bay, the supply of latent heat continues and at the stage of maximum intensity, the LHF is increased to reach its maximum value. The MSWS associated with a TC increase with the increase of LHF. At the time of landfall, the distribution of LHF shows that there is a band of LHF around the center of the system, and maximum LHF is determined in the northwest part of the system. The maximum value is roughly more than 1200, 1100, 800-900, and 600-700 W m^{-2} for 96, 72, 48, and 24-hour simulations respectively.

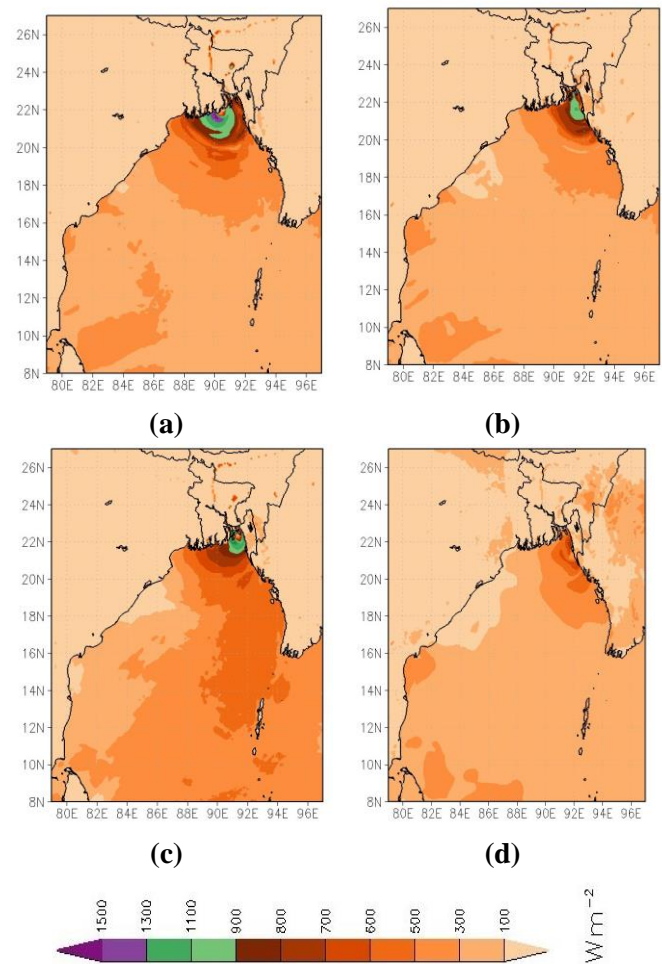


Fig. 9. The spatial distribution of LHF based on 0000 UTC of (a) 27, (b) 28, (c) 29, and (d) 30 May, 2017 respectively.

The positive values of LHF indicate the gain of energy from the ocean surface to the atmosphere. The maximum source of latent heat along the northwest part of the system makes the wind in this region the strongest which is supported by the strong upward motion along the northwest sector of the TC.

Analysis of Temperature at 2m Height

The model simulated temperature ($^{\circ}\text{C}$) at the 2-meter height of the TC Mora at (the time of model simulated landfall) 2300 UTC of 29th May, 0100 UTC, 0100 UTC, 0200 UTC of 30th May 2017 for 96, 72, 48, and 24-hours simulations are presented in Fig. 10 (a-d) respectively. According to the analysis of the simulated temperature at this level, the system center's temperature at the time of landfall for 96, 72, 48, and 24-hour simulations is determined to be around 27-35 $^{\circ}\text{C}$. The temperature continued to decline after landfall, according to the analysis. The simulated temperature was significantly lower in the southern part of Bangladesh as well as the surrounding regions. It is found that the temperature decreases to 24-27 $^{\circ}\text{C}$. This is due to

heavy rainfall occurring around the time of TC Mora's landfall, which has dropped the temperature and is highly conducive to the development of rainfall. The declining pattern of temperature has been reasonably simulated by the WRF model.

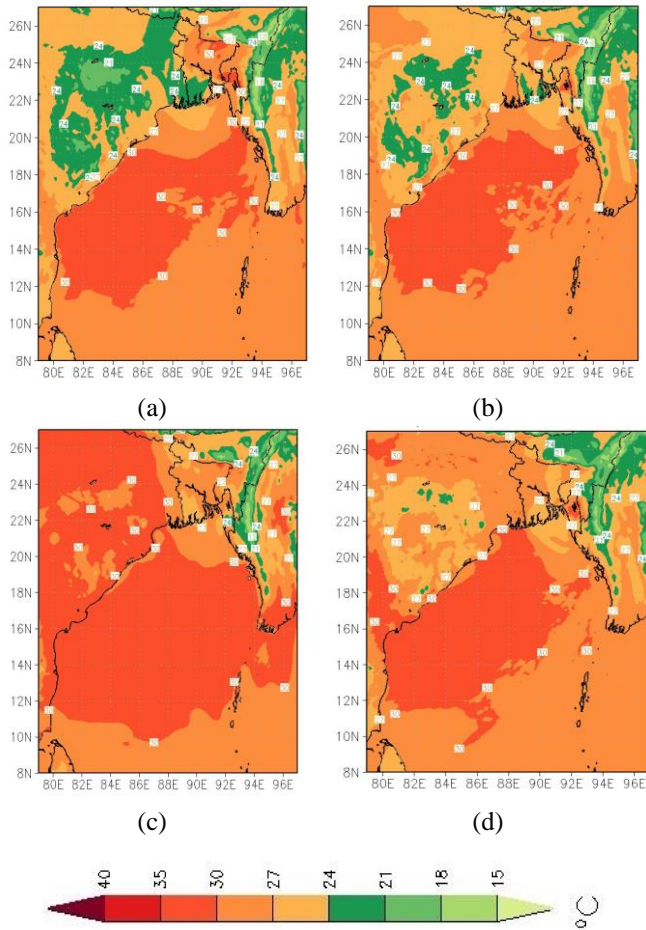


Fig. 10. The spatial distribution of temperature based on 0000 UTC of (a) 27, (b) 28, (c) 29, and (d) 30 May, 2017 respectively.

Analysis of Rainfall

The model simulated rainfall (mm) of the TC Mora at (the time of model simulated landfall) 2300 UTC of 29th May, 0100 UTC, 0100 UTC, 0200 UTC of 30th May 2017 for 96, 72, 48, and 24-hour simulations are shown in Fig. 11(a-d) respectively. The simulated rainfall is assessed to be very heavy, ranging between 90-180 mm across the southern part of Bangladesh and adjacent regions. According to the findings, there was heavy impact rainfall over the region of southern Bangladesh, but comparatively low rainfall across the remaining country.

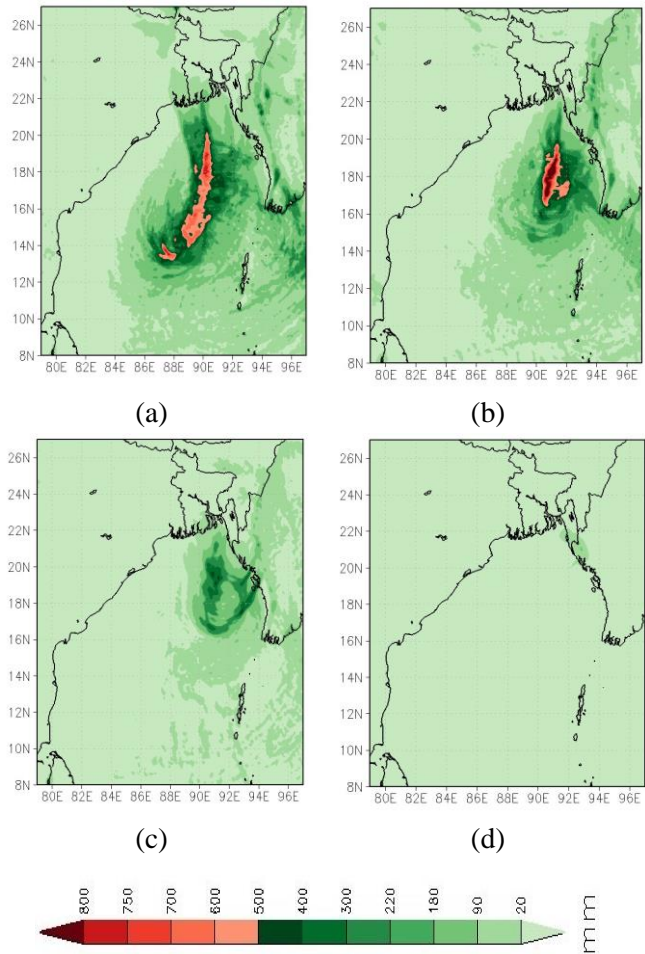


Fig. 11. The spatial distribution of Rainfall based on 0000 UTC of (a) 27, (b) 28, (c) 29, and (d) 30 May, 2017 respectively.

The highest rainfall is determined in the southwest portion of the cyclone center. From the spatial distribution of simulated rainfall, it is found that the southeast sector experiences the primary high amount of rainfall. Then the TC moved north-eastwards and a secondary high amount of rainfall occurs over the southwest sector of the system center. Fig. 12(a-d) represents a comparison of the model-predicted 24-hour accumulated rainfall and the observed rainfall of BMD at seven different stations on May 30, 2017 (on the day of landfall). The model overestimates the amount of rainfall compared to the observation at almost all of the considered stations for the 96, 72, 48, and 24-hour model runs.

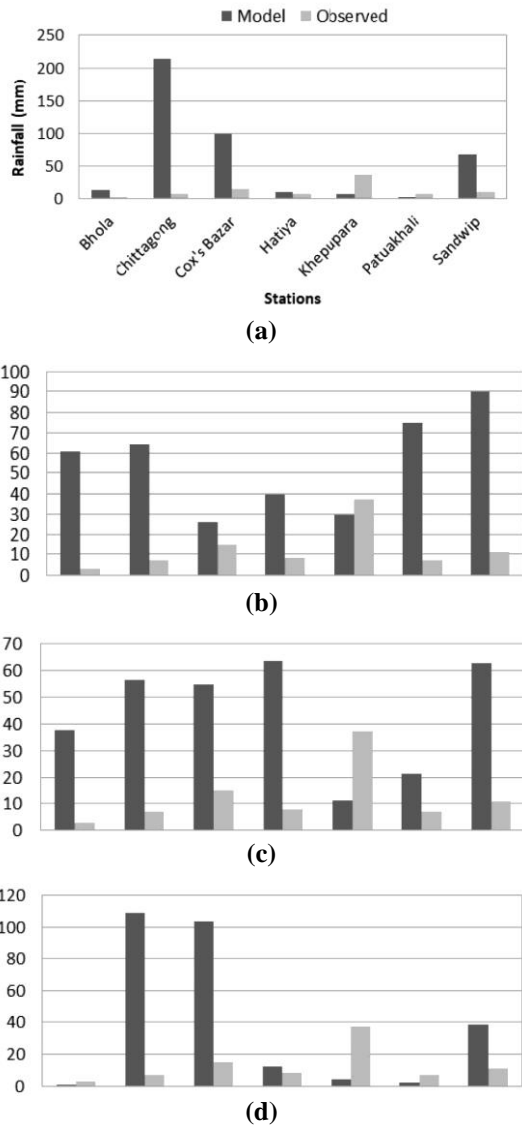


Fig. 12. Comparison of the model predicted 24-hour accumulated rainfall (mm) and the observed rainfall (BMD) at different stations on 30th May, 2017 (on the day of landfall) for (a) 96 (b) 72 (c) 48 (d) 24-hour simulations, respectively.

Track Analysis

The observed track of TC Mora is presented in Fig. 13 (a-c) with the model predicted track based on the initial conditions of 0000 UTC on the 28th, 29th, and 30th May,

2017 respectively. As cyclone Mora's lifetime was only around 72 hours, observed datasets for 96 hours are not available. As a result, the simulated 96-hour track has not been compared with the observation.

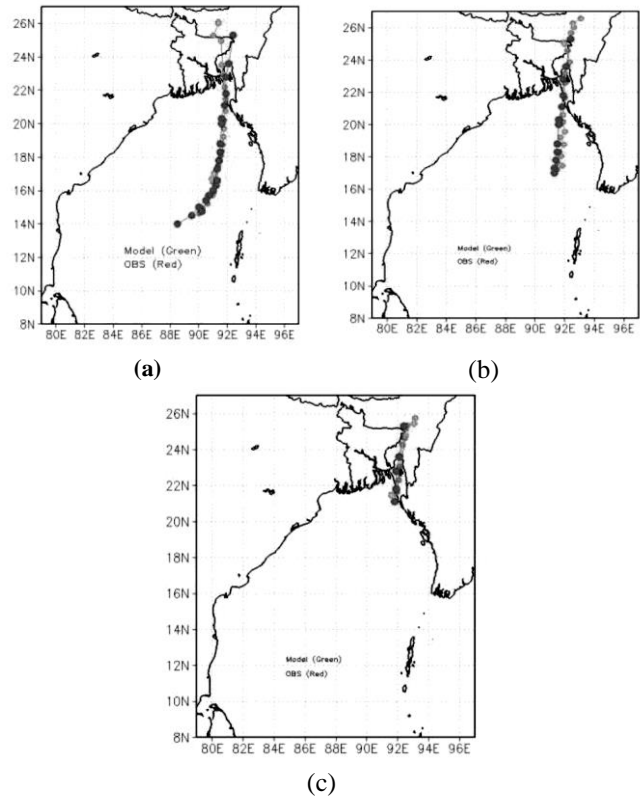


Fig. 13. The simulated track (green) along with the observed track (red) based on (a) 72, (b) 48, and (c) 24-hour simulations respectively.

The Figures clearly show that the predicted tracks are identical to the observed tracks. The model has generated the system's northeastward movement for each of the 72, 48, and 24-hour simulations, as seen by the observed track. Therefore, the model has simulated the direction of motion of the system very well with a considerable error in the landfall position prediction. It can be concluded that even 72 and 48 hours, the model has generated the track of the SCS Mora efficiently with some time and position errors. The simulated landfall position and time errors are analyzed in assessing the WRF model's performance. Table 2 includes the summary of the findings.

Table 2. Landfall position and time error of Cyclone Mora

Time (UTC)/Base Date	Forecast hours	Simulated Results		Actual Landfall		Forecast Error	
		Position	Time	Position	Time	Distance (km)	Time (hours)
00/ 27 May	96	21.97 ⁰ N 90.33 ⁰ E	23/ 29 May			174	4 hours E
00/ 28 May	72	21.78 ⁰ N 91.82 ⁰ E	01/ 30 May	22 ⁰ N	0400-0500 UTC	26	3 hours E
00/ 29 May	48	21.41 ⁰ N 91.98 ⁰ E	01/ 30 May	91.9 ⁰ E	30 May	65	3 hours E
00/ 30 May	24	21.62 ⁰ N 91.95 ⁰ E	02/ 30 May			42	2 hours E

- E and 23/29 May indicate earlier the landfall of cyclone Mora and 2300 UTC of 29 May.

V. Conclusion and Future Prospects

In this study, the simulated MCP of SCS Mora is about 935, 955, 972, and 977 hPa for 96-, 72-, 48- and 24-hour simulations respectively. The IMD ECP was 978 hPa, indicating that the model overestimated the change in pressure.

The magnitude of MSWS changes depending on the initial conditions-based simulations. The asymmetric structure of the cyclone has been well captured by several magnitudes of zonal and meridional winds at different sectors of the system.

The model has reasonably simulated the track and timing of landfall of TC Mora even in the 96-hour prediction. The findings also suggest that as prediction time decreases, landfall efficiency improves.

The current study performed the sensitivity test using a single cumulus physics scheme. However, more cases will be examined in the future to analyze the impact of several cumulus physics schemes on simulating TCs over the BoB. The WRF model has been utilized in a single domain with the HR of 10 km. The model output has not been assessed for variations in domain size. More cases will be studied in the future to find out the impact of domain size on various cases. The present study uses a single micro-physics scheme. More cases will be analyzed in the future to analyze the impact of various micro-physics schemes on the accuracy of simulating TCs over the BoB. Such studies will help develop a combination of physics schemes in the WRF model to study TCs (over BoB) more efficiently. Conducting experiments on the formation, intensification,

and translational speed of TCs over the BoB is also essential.

References

1. Kanase, R. D. and P. S. Salvekar, 2014. Study of Weak Intensity Cyclones over the Bay of Bengal Using WRF Model. *Atmospheric and Climate Sciences*, **4**, 534-548.
2. Quader, M. A., A. U. Khan, and M. Kervyn, 2017. Assessing Risks from Cyclones for Human Lives and Livelihoods in the Coastal Region of Bangladesh. *Int. J. Environ. Res. Public Health*, **14**(8).
3. Wahiduzzaman, M., and A. Yeasmin, 2019. Statistical forecasting of tropical cyclone landfall activities over the North Indian Ocean rim countries. *Atmos. Res.*, **227**, 89-100.
4. Gray, W. M., 1968. Global view of the origin of tropical disturbances and storms. *Mon. Wea. Rev.*, **96**(10), 669-700.
5. Alam, M. M., 2020. Sensitivity study of planetary boundary layer parameterization schemes for the simulation of tropical cyclone 'Fani' over the Bay of Bengal using high-resolution WRF-ARW model. *Journal of Engineering Science*, **11**(2), 1-18.
6. Shultz, J. M., J. Russell, and Z. Espinel, 2005. Epidemiology of tropical cyclones: The dynamics of disaster, disease, and development. *Epidemiologic Reviews*, **27**, 21-35.
7. Pattanaik, S., and U. C. Mohanty, 2008. A comparative study on the performance of MM5 and WRF models in simulation of tropical cyclones over Indian seas. *Current Sci.*, **95**(7), 923-936.
8. Hossain, M. S., M. A. Samad, S. M. A. Hossen, S. M. Q. Hassan, and M. A. K. Malliak, 2021. The Efficacy of the WRF-ARW Model in the Genesis and Intensity Forecast of

- Tropical Cyclone Fani over the Bay of Bengal. *Journal of Engineering Science*, **12**(3), 85-100.
9. Islam, M. J., A. Imran, I. M. Syed, S. Q. Hassan, and M. I. Ali, 2019. The Sensitivity of Microphysical Parameterization Schemes on the Prediction of Tropical Cyclone Mora Over the Bay of Bengal using WRF-ARW Model, *Dhaka Univ. J. Sci.*, **67**(1), 33–40.
 10. Hossain, M. S., M. A. Samad, M. R. Sultana, M. A. K. Malliak, and M. J. Uddin, 2021. Track and Landfall Characteristics of Very Severe Cyclonic Storm Fani over the Bay of Bengal using WRF Model. *Dhaka Univ. J. Sci.*, **69**(2), 101-108.
 11. Frank, W. M., 1983. The cumulus parameterization problem. *Mon. Wea. Rev.*, **111**, 1859-1871.
 12. Wang, Y., and C. C. Wu, 2004. Current understanding of tropical cyclone structure and intensity changes -A review. *Meteor. Atmos. Phys.*, **87**, 257-278.
 13. Hill, K. A., and G. M., Lackmann, 2009. Influence of environmental humidity on tropical cyclone size. *Mon. Wea. Rev.*, **137**, 3294-3315.
 14. Moon, Y., and D. S. Nolan, 2010. The dynamic response of the hurricane wind led to spiral rainband heating. *J. Atmos. Sci.*, **67**, 1779-1805.
 15. Deshpande, M. S., S. Pattnaik, and P. S. Salvekar, 2012. Impact of cloud parameterization on the numerical simulation of a super cyclone. *Ann. Geophys.*, **30**, 775-795.
 16. Mohanty, U. C., K. K. Osuri, A. Routray, M. Mohapatra and S. Pattanayak, 2010. Simulation of Bay of Bengal tropical cyclones with WRF Modeling system: Impact of Initial Value and Boundary Conditions. *Marine Geodesy*, **33**, 294-314.
 17. Akhter, M. A. E., M. M. Alam and M. A. K. Mallik, 2016. Simulation of the structure and track of the tropical cyclone Rashmi using numerical models. *Dewdrop*, **2**(1), 60-74.
 18. Patra, K. P., M. S. Santhanam, K. V. J. Potty, M. Tewari, and P. L. S. Rao, 2000. Simulation of tropical cyclones using regional weather prediction models. *Current Sci.*, **79**, 1, 70-78.
 19. Uddin, M. J., M. A. Samad, M. A. K. Mallik, 2021. Impact of Horizontal Grid Resolutions for Thunderstorms Simulation over Bangladesh Using WRF-ARW Model. *Dhaka University Journal of Science*, **69**(1), 43-51.
 20. Hossain, M. S., M. A. Samad, M. S. Hossain, S. M. A. Hossen, M. A. Islam, and S. M. Q. Hassan, 2022. The Sensitivity of Initial Condition and Horizontal Resolution on Simulation of Tropical Cyclone Amphan over the Bay of Bengal using WRF-ARW Model. *Dhaka University Journal of Science*, **69**(3), 202-211.
 21. Mayumi, O., 2016. Disaster Risk Financing in Bangladesh. ADB South Asia working paper series, **46**, 1-35. Available at: <https://www.adb.org/sites/default/files/publication/198561/sawp-046.pdf>
 22. RMSC, 2017. *Severe Cyclonic Storm, 'MORA' over the Bay of Bengal (28-31 May, 2017): A Report*; Cyclone Warning Division, India Meteorological Department, New Delhi, India. Available at: https://rsmcnewdelhi.imd.gov.in/uploads/report/26/26_385d6a_mora.pdf
 23. Kessler, E., 1969. On the distribution and continuity of water substance in atmospheric circulations. *Meteor. Monogr.*, **32**, 1-48. https://doi.org/10.1007/978-1-935704-36-2_1
 24. Kain, J. S., 2004. The Kain–Fritsch Convective Parameterization, An Update. *J. Appl. Meteor.*, **43**, 170-181.
 25. Hong, S. Y., Y. Noh, and J. Dudhia, 2006. A new vertical diffusion package with an explicit treatment of entrainment processes. *Mon. Wea. Rev.*, **134**(9), 2318-2341.
 26. Jimenez, P. A., J. Dudhia, F. G. Rouco, J. Navarro, J. P. Montavez, and E. B. Bustamante, 2012. A revised scheme for the WRF surface layer formulation. *Mon. Wea. Rev.*, **140**, 898-918.
 27. Tewari, M. F., C. W. Wang, J. Dudhia, M. A. LeMone, E. Mitchell, M. Ek, G. Gayno, J. Wegiel, and R. H. Cuenca, 2004. Implementation and verification of the unified NOAA land surface model in the WRF model. 20th conference on weather analysis and forecasting/16th conference on numerical weather prediction, 11-15.
 28. Dudhia, J., 1989. Numerical study of convection observed during the Winter Monsoon Experiment using a mesoscale two–dimensional model. *J. Atmos. Sci.*, **46**, 3077–3107.
 29. Mlawer, E. J., S. T. Taubman, P. D. Brown, M. J. Iacono, and S. A. Clough, 1997. Radiative transfer for inhomogeneous atmospheres: RRTM, a validated correlated–k model for the long wave. *J. Geophys. Res.*, **102**, 16663-16682.